SURFACE ADJUSTMENT OF BIOCHAR BY CO_2 GASIFICATION UNDER FIXED AND FLUIDIZED BED CONDITIONS

Florian J. Müller[1]*, Camila Rodríguez M.[1], Eugen Schöfbänker[1], Franz Winter[1]

Technische Universität Wien, Institute of Chemical, Environmental and Bioscience Engineering. Getreidemarkt 9/166, 1060 Wien, Austria

*E-mail: *florian.johann.mueller@tuwien.ac.at*

Abstract

This paper explores how torrefaction and CO_2 gasification can be combined to create biochar with a high surface area from *Pinus sylvestris* wood pellets. Raw pellets were pretreated in a torrefaction process at 300 °C before conducting biomass CO_2 gasification experiments under various operating conditions. Gasification was performed under fixed and fluidized bed conditions at temperatures between 800 to 900 °C and biomass residence times of 15 or 25 minutes. Biomass burn-off and BET surface areas were analyzed individually and combined to determine the surface yield per raw *Pinus sylvestris* feedstock. Higher temperatures, higher biomass residence times, and fixed bed conditions increased burn-off and BET surface areas up to 798 m²/g. Surface yield per raw biomass was instead found to be the highest from fluidized bed experiments, which yielded around 100 $m^2/g_{feedstock}$ after gasification at 850 to 900 °C.

1. Introduction

Biomass CO_2 gasification is a carbon capture and utilization technology producing CO-rich gas [1]. Potential applications of such gas are for iron ore reduction in a direct reduced ironmaking shaft furnace [2] or, if sustainable hydrogen is added, as a synthesis gas for producing renewable chemicals and energy carriers [3]. If no oxygen is fed to the gasification reaction, biomass is often not fully converted, and the residual char is frequently used for energy generation [5]. The specific surface areas of typical biochars (from 0.1 to 500 m²/g) make them suited for applications like soil amendment [7] and to restore degraded sites [8]. Activated biochars with high specific surface areas of 200 to 2500 m²/g can be produced from various biomass feedstocks by thermochemical treatment and can be used for higher-value applications like catalysis, electrochemistry, or energy storage [9]. An ongoing research project on phytoremediation at TU Wien investigates the encapsulation of heavy metals in biochar. In this project, one investigated process route is a multi-stage process consisting of a torrefaction process at mild temperatures as pretreatment and a CO_2 gasification step for surface activation at high temperatures. This paper investigates the influence of CO_2 gasification operating conditions on the surface characteristics of biochar.

1.1. State of the art on surface adjustment by gasification

The manufacturing process of activated biochar generally consists of a carbonization step, creating a biochar structure with pores that are often blocked by tar compounds, and an activation step, during which these blockages are removed and the pores are widened [10]. This activation step can be realized by adding chemicals before thermal or physical activation through gasification, where oxidizing gases penetrate the structure at temperatures between 700 and 1000 °C [11]. The characteristics of the final product depend mainly on feedstock composition and process conditions such as heating rate, temperature, and residence time [12].

CO_2 and H_2O are the most common gasification agents for producing high surface area biochars because their endothermic reactions can be controlled well [13]. Chang et al. reported on the gasification of corn cob agro-waste that at 900 °C higher Brunauer-Emmett-Teller (BET) surface areas and total pore volumes were found with CO_2 as gasification agent

compared to steam (1705 vs. 1063 m²/g; 0.884 vs. 0.536 cm³/g) [14]. The opposite trend was reported at 800 °C (670 vs. 998 m²/g; 0.342 vs. 0.511 cm³/g), which can be attributed to the higher reaction rate for the steam-carbon reaction with H_2O compared to the Boudouard reaction with CO_2 [13]. Pallarés et al. reported a similar trend reversion when they studied the activation of barley straw after carbonization via pyrolysis at 500 °C [11]. BET surface area and pore volume were higher from CO_2 gasification at 800 °C (789 vs. 534 m²/g; 0.3495 vs. 0.2576 cm³/g), but higher surface area was found for steam gasification at 700 °C (211 vs. 552 m²/g). Additionally, Ngernyen et al. reported a linear increase in burn-off values and BET surface area with increasing activation time between 60 and 300 minutes for the CO_2 activation of Eucalyptus and Wattle wood [15].
Based on the presented literature, activation time and temperature were selected to investigate *Pinus sylvestris* pellets' surface evolution during CO_2 gasification. Additionally, the experiments were performed under fixed and fluidized bed conditions to examine if this would lead to different results, e.g., from differences in heat transfer.

2. Materials and methods

2.1. Experimental design

Pellets with a diameter of approximately 4 mm and varying lengths between 5 to 20 mm were produced from a mixture of *Pinus sylvestris* needles and branches (Table 1). The pellets were subjected to a pre-treatment phase by torrefaction and further activation by gasification. The torrefaction process was performed under an N_2 atmosphere and fixed bed conditions in a separate reactor with an inner diameter of 53 mm. This larger reactor was used because it enabled the production of torrefied intermediate products for all gasification experiments in a single batch. The pellets were kept at 300 °C for 45 minutes under a nitrogen flow of 0.8 Nm³/h. Quartz sand with a density of 2650 kg/m³ and a particle mean diameter determined by sieving analysis at 370 µm was used as bed material during fluidized bed experiments. CO_2 and N_2 from gas bottles were used as gaseous feed.

Table 1: Elemental analysis of raw Pinus sylvestris pellets

	Water content	C	H	N	S	O
wt%	4.6	50.0	6.9	1.1	0.7	41.3

Torrefied biochar was activated by gasification with CO_2 in a stainless-steel batch reactor with an inner diameter of 38 mm (Figure 1a). Two external half-shells electrically heated the reactor (Figure 1b). Temperatures were measured by thermocouples type K. A gas mixture of 1.6 NL/min N_2 and 0.4 NL/min CO_2 was supplied to the reactor and controlled by mass flow controllers for all experiments. Gas entered the reactor through an empty preheating section before a Quartz glass frit distributed the gas evenly into the upper section, where the activation process was carried out (reaction zone). Fuel was inserted into the reaction zone batch-wise. It was placed into a metal cage with a mesh size of approximately 500 µm, which was used for extracting the activated biochar after the experiment. Fuel was added after the reactor had reached its desired temperature.

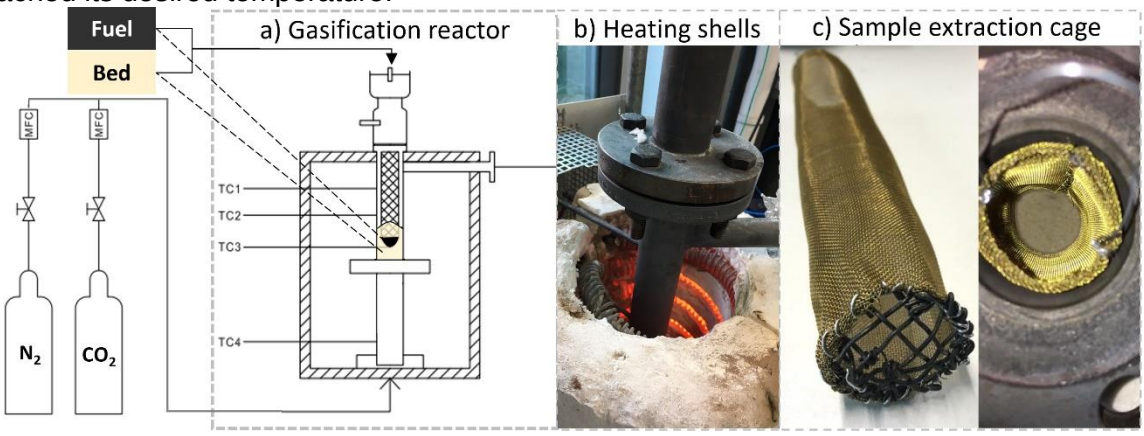

Figure 1:a) Gasification reactor schematic layout, b) Reactor with heating, c) Sample extraction cage

For fluidized bed experiments, fuel was submerged in Quartz sand. Fluidization equations proposed by Grace [16], Wen, and Yu [17] were used to calculate that the selected feed gas flow rate of 2.0 NL/min resulted in around 5 times the minimum fluidization velocity. Therefore, the fluidized bed conditions were achieved by forming a bubbling fluidized bed from Quartz sand particles around the fuel in the sample extraction cage (Figure 1c).
A four-step procedure was followed after the activation time to stop reactions and freeze the surface state of biochar: 1. The electrical heating was turned off, 2. CO_2 was no longer fed to the reactor (only N_2), 3. 50 mL of Quartz sand at room temperature was fed through the ball valve lock to lower the temperature in the reactor, and 4. A part of the insulation was removed to cool down the biochar faster. After the reactor had cooled down, the activated biochar samples were removed by carefully lifting the cage.
A list of the selected experimental conditions for activation is given in Table 2.

Table 2: Investigated gasification conditions

Name	Fluidization		Temperature			Activation time	
	Fluidized bed	Fixed bed	800°C	850°C	900°C	15 min	25 min
E1		X	X			X	
E2		X		X		X	
E3		X			X	X	
E4		X	X				X
E5		X		X			X
E6		X			X		X
E7	X		X			X	
E8	X			X		X	
E9	X				X	X	
E10	X		X				X
E11	X			X			X
E12	X				X		X

2.2. Sample characterization

The weight loss of the solid samples during processing is described by the burn-off value (*b*), which is formed from the weight before the conversion step (w_0) and the weight of the final product (w_f); see Eq. 1.

$$b = \frac{w_0 - w_f}{w_0} \qquad \text{Eq. 1}$$

Nitrogen adsorption isotherms for surface characterization were measured using an ASAP 2020 Plus adsorption analyzer by Micromeritics for the torrefied biochar and a Belsorp Max G by Microtrac Retsch for samples after activation. These measurements were also used to determine the total pore volume. Before measurement, the activated samples were degassed under vacuum in a Belprep Vac degassing station for 24 hours at 150°C, which is suggested as degassing temperature in the European Biochar Certification [18]. The torrefied sample was degassed at 200 °C for 4 hours. Isotherm data were used to calculate a specific surface area a_{BET} following the proposed method by Brunauer-Emmett-Teller (BET) [19]. Guidelines for applying this method to microporous materials, as given in Annex C of DIN ISO 9277:2014-01, were followed for activated samples. These guidelines were proposed by Rouquerol et al. [20] and are as follows:

- C must be positive
- Application of the BET equation must be limited to the range where the term $V(1-P/P_0)$ continuously increases with P/P_0
- The P/P_0 value corresponding to the monolayer volume should be within the selected BET range.

Two further criteria were followed to select the appropriate range for multi-point BET in this analyzer:

- The first point of the fit must be at least $1 \cdot 10^{-3}$ Pa following pressure measurement sensitivity.

- The last point of the fit is chosen to achieve the highest correlation coefficient between data and fit.

Furthermore, light microscopy using a Keyence VHX-S650E and a VH-ZST dual zoom objective and scanning electron microscopy (SEM) were used to evaluate surface adjustments. Samples were sputtered with gold before analysis in a COXEM EM-30 Plus microscope.
Increasing the surface area further and further might not bring additional benefits for some applications, which might, for example, only need 500 m²/g to reach process demands. In such cases, optimal operating conditions to produce biochar could be identified by considering both a_{BET} and *b*. A surface yield parameter (*y)* is proposed that relates the final biochar surface area a_{BET} to the mass of *Pinus sylvestris* feedstock used for producing this biochar (Eq. 2). Higher *y* values indicate that higher total surface area is produced per mass of raw feedstock.

$$y = a_{BET} \cdot \left(1 - b_{torrefaction}\right) \cdot \left(1 - b_{gasification}\right) \quad \text{Eq. 2}$$

3. Results and discussion

3.1. Biomass conversion

A burn-off value (*b*) of 32.64 % was recorded during torrefaction. The torrefied pellets were dark brown and softer in texture compared to the raw pellets, suggesting a slight surface degradation and the presence of tar in the pore structures. Investigations by SEM at various magnifications from x50 to x2000 confirmed that the pore structure remained relatively closed after torrefaction (Figure 2). Small hollows and irregularities were visible in the raw and torrefied samples due to the pelletization process mixing needles and branches. At the process temperature of 300 °C and under constant nitrogen flow, this weight loss was likely caused by drying and the decomposition of hemicellulose [13].

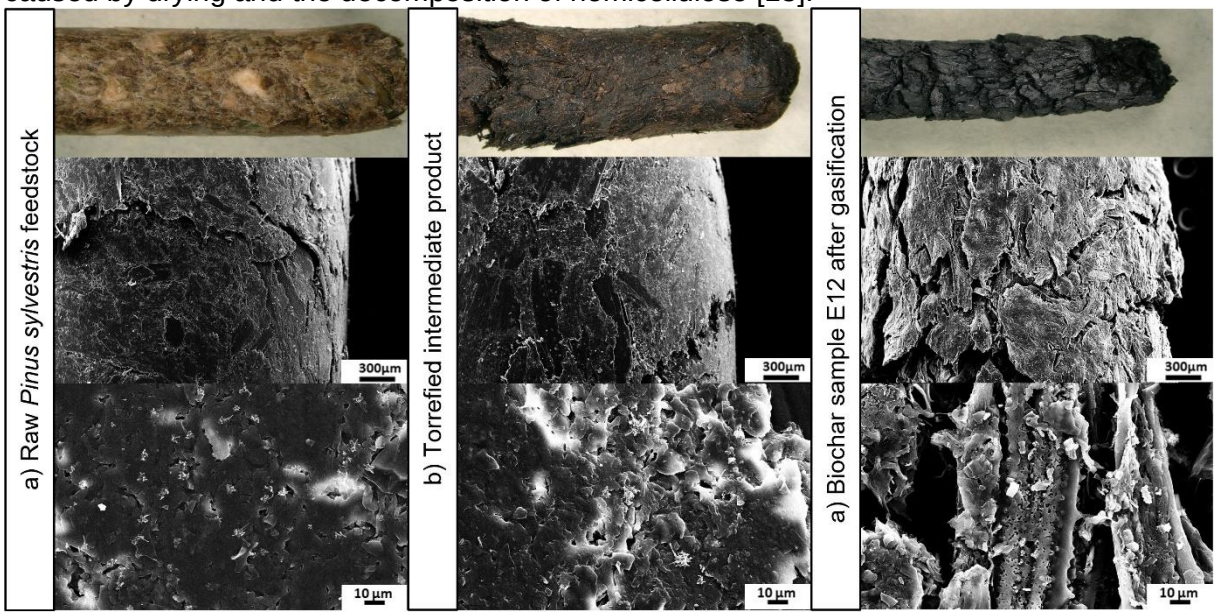

Figure 2: Evolution of Pinus sylvestris pellets during thermal processing investigated by light and scanning electron microscopy (x50, x1000 magnifications).

Significant further weight losses were recorded during gasification with CO_2 (Figure 3). Burn-off was calculated relative to the torrefied intermediate product. Biochar pellets were black and brittle after gasification, and their diameter had decreased by 25 % on average. Morphological examination under light microscopy and SEM revealed a surge in fragmentations and the development of both, narrow and larger pore structures that were not there before gasification. The inner structure showed the presence of channels and hollow areas next to each other, which might be related to solid-gas reactions with CO_2.

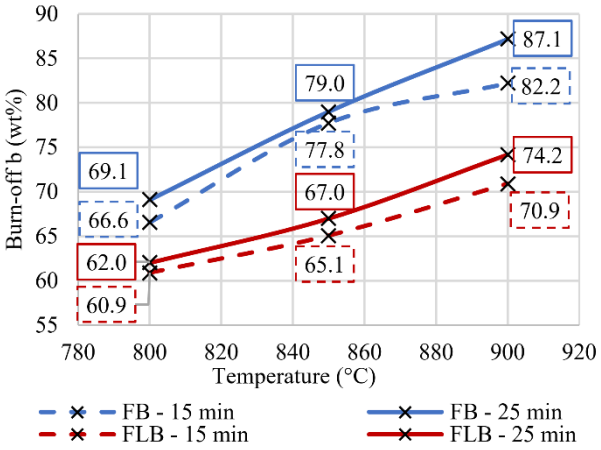

Figure 3: Burn-off during CO_2 gasification under various conditions. FB=Fixed bed; FLB=Fluidized bed.

The increase in biochar residence time from 15 to 25 minutes increased burn-off for fluidized bed and fixed beds experiments. Burn-off was also increased at higher temperatures. Devolatilization at high temperatures is a fast process [6], suggesting that the burn-off increase at longer residence times was a result of ongoing gas-solid reactions. Temperatures exceeding 800 °C lead to the pyrolytic decomposition of more stable biomass components [22] and also favor fixed carbon conversion by gas-solid reactions, mainly the Boudouard reaction [1]. Therefore, the increase in burn-off at higher temperatures can be attributed to a mixture of pyrolytic decomposition and reactions with the gasification agent CO_2.
Burn-off values across all temperatures and residence times were higher under fixed bed than under fluidized bed conditions. Various factors could influence this result, e.g., an inhibition effect of silicon in the bed material could have lowered the biomass conversion under fluidized bed conditions [1][21]. Another reason could be lower fuel-gas contact times under fluidized bed conditions, due to inconsistent fluidization and effects like gas channeling around the sample cage. Differences in heat transfer from the external heating shell to the thermocouples outside the sample extraction cage and biomass inside the cage could also lead to this result because the cage could have decreased heat transfer from the heating to the sample by hindering radial mixing. As a result, the samples' actual temperature could have been higher under fixed bed than under fluidized bed conditions.

3.2. BET surface

Multi-point fitting data, calculated BET surface areas, and total pore volumes are given in Table 3. Correlation coefficients between isotherm measurement data and selected multi-point fits were at least 0.9981.

Table 3: Surface characterization data from BET surface measurement by N_2 adsorption

Name	p/p_0		C	Isotherm data points in the fitting range	BET surface area (m^2/g)	Total pore volume (cm^3/g)
	Low point	High point				
Torref.	1.01E-02	0.07	46	4	0.65	9E-04
E1	1.16E-03	0.23	261	16	201	0.09
E2	1.12E-03	0.20	812	30	387	0.17
E3	1.76E-03	0.05	2902	8	608	0.25
E4	1.07E-03	0.14	1177	9	193	0.09
E5	2.13E-03	0.04	3702	6	498	0.20
E6	1.39E-03	0.05	1913	12	798	0.34
E7	3.28E-03	0.10	645	6	55	0.03
E8	1.10E-03	0.20	796	24	340	0.15
E9	1.03E-03	0.04	3811	8	482	0.20
E10	4.76E-03	0.14	655	9	240	0.11
E11	1.76E-03	0.03	4088	5	451	0.18
E12	1.44E-03	0.04	3472	7	560	0.23

Surface areas and total pore volume are orders of magnitude higher for biochar samples after CO_2 gasification. BET surface area and total pore volume increased with higher burn-off values. Samples prepared under fixed bed conditions generally showed higher surface areas and pore volumes than samples prepared under fluidized bed conditions. Both values were increased for samples prepared at higher gasification temperatures and solid residence times. The surface area measured after 25 minutes of fixed bed operation was around 4 times as much as the surface area after treatment at 800 °C under otherwise equivalent conditions, showing that temperature had a high impact.

This indicates two things: First, heat transfer problems under fluidized bed conditions might also explain the differences observed in surface area and pore volume compared to fixed bed conditions. Second, since the difference between 800 and 900 °C significantly impacts the thermodynamic equilibrium and reaction kinetics of the Boudouard reaction in biomass CO_2 gasification [1], these results suggest that surface area growth is largely caused by the Boudouard reaction.

While these results suggest fixed bed conditions, long solid residence times, and high temperatures for producing biochar with a high BET surface area, fixed bed conditions did not yield the highest surface area per mass of raw feedstock. Figure 4 compares the BET surface area results side-by-side with the surface yield. The second metric suggests that the yield of surface area per mass of feedstock was higher from gasification under fluidized bed conditions. Around 100 $m^2/g_{feedstock}$ are found for gasification under fluidized bed conditions and at 850 °C or 900 °C. Since the BET surface area measured for these samples was also near or above 500 m^2/g, fluidized bed operation seems to have an edge in yield for applications that do not need BET surface areas over 500 m^2/g.

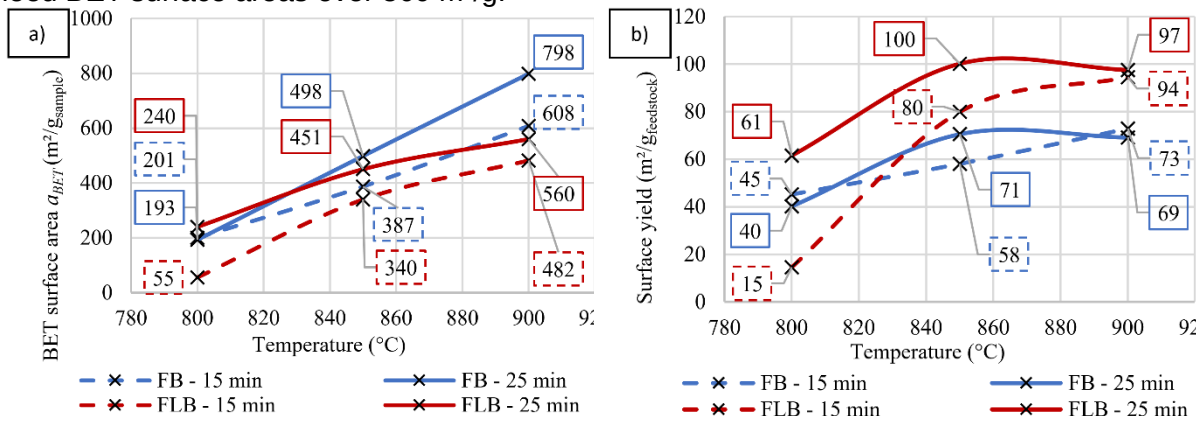

Figure 4: a) BET surface area of biochar, b) Surface yield from raw biomass to biochar.

4. Conclusion

The combination of torrefaction pretreatment and biomass CO_2 gasification produced biochar with a high surface area. CO_2 gasification increased BET surface areas by two to three orders of magnitude compared to the torrefied intermediate product. Higher temperatures and solid residence times lead to higher BET surface areas, burn-off, and surface yields. While fixed bed conditions were used to produce the highest BET surface areas and pore volumes in this work, fluidized bed conditions yielded more total surface area per raw feedstock due to lower burn-off values during gasification. Therefore, fluidized bed gasification should be considered if the biochar meets the application's demands. Further research could help to determine if the observed differences in burn-off are a system-specific result of this experimental setup. Since high temperatures and solid residence times are also favorable for utilizing CO_2 in this process, using biomass CO_2 gasification as a CCU process and for producing high-quality biochar is promising.

Acknowledgment

This study was carried out within the doctoral college *CO_2Refinery* at TU Wien and was part of the research project *Processes for metal-to-char encapsulation* (I 5404) funded under the grant-DOI 10.55776/I5404. N. Steinacher and J. Piotrowska of TU Wien, and A. Korus of Silesian University of Technology are acknowledged for their help with surface analysis.

References

[1] F. J. Müller *et al.*, "CO2 conversion to CO by fluidized bed biomass gasification : Analysis of operational parameters," *Journal of CO2 Utilization*, vol. 81, no. March 2024, 2024, doi: 10.1016/j.jcou.2024.102706.

[2] A. Nurdiawati, I. N. Zaini, W. Wei, R. Gyllenram, W. Yang, and P. Samuelsson, "Towards fossil-free steel: Life cycle assessment of biosyngas-based direct reduced iron (DRI) production process," *J Clean Prod*, vol. 393, no. January, p. 136262, 2023, doi: 10.1016/j.jclepro.2023.136262.

[3] Y. H. Chan, S. N. F. Syed Abdul Rahman, H. M. Lahuri, and A. Khalid, "Recent progress on CO-rich syngas production via CO2 gasification of various wastes: A critical review on efficiency, challenges and outlook," *Environmental Pollution*, vol. 278, pp. 1–16, 2021, doi: 10.1016/j.envpol.2021.116843.

[4] A. Lampropoulos *et al.*, "Effect of Olive Kernel thermal treatment (torrefaction vs. slow pyrolysis) on the physicochemical characteristics and the CO2 or H2O gasification performance of as-prepared biochars," *International Journal of Hydrogen Energy*, vol. 46, no. 57. pp. 29126–29141, 2021. doi: 10.1016/j.ijhydene.2020.11.230.

[5] A. M. Mauerhofer *et al.*, "Conversion of CO2 during the DFB biomass gasification process," *Biomass Convers Biorefin*, vol. 11, no. 1, pp. 15–27, 2021, doi: 10.1007/s13399-020-00822-x.

[6] P. Lahijani, Z. A. Zainal, M. Mohammadi, and A. R. Mohamed, "Conversion of the greenhouse gas CO2 to the fuel gas CO via the Boudouard reaction: A review," *Renewable and Sustainable Energy Reviews*, vol. 41, pp. 615–632, 2015, doi: 10.1016/j.rser.2014.08.034.

[7] B. M. Ohsowski, K. Dunfield, J. N. Klironomos, and M. M. Hart, "Plant response to biochar, compost, and mycorrhizal fungal amendments in post-mine sandpits," *Restor Ecol*, vol. 26, no. 1, pp. 63–72, Jan. 2018, doi: 10.1111/rec.12528.

[8] M. Ahmad, S. S. Lee, S. E. Lee, M. I. Al-Wabel, D. C. W. Tsang, and Y. S. Ok, "Biochar-induced changes in soil properties affected immobilization/mobilization of metals/metalloids in contaminated soils," *J Soils Sediments*, vol. 17, no. 3, pp. 717–730, Mar. 2017, doi: 10.1007/s11368-015-1339-4.

[9] F. L. Braghiroli, H. Bouafif, C. M. Neculita, and A. Koubaa, "Influence of Pyro-Gasification and Activation Conditions on the Porosity of Activated Biochars: A Literature Review," *Waste and Biomass Valorization*, vol. 11, no. 9. Springer, pp. 5079–5098, Sep. 01, 2020. doi: 10.1007/s12649-019-00797-5.

[10] V. Benedetti, F. Patuzzi, and M. Baratieri, "Gasification Char as a Potential Substitute of Activated Carbon in Adsorption Applications," in *Energy Procedia*, Elsevier Ltd, 2017, pp. 712–717. doi: 10.1016/j.egypro.2017.03.380.

[11] J. Pallarés, A. González-Cencerrado, and I. Arauzo, "Production and characterization of activated carbon from barley straw by physical activation with carbon dioxide and steam," *Biomass Bioenergy*, vol. 115, pp. 64–73, Aug. 2018, doi: 10.1016/j.biombioe.2018.04.015.

[12] A. Korus, "Investigation of Tar Conversion Over Biomass Char," University of Lincoln, 2019. doi: https://doi.org/10.24385/lincoln.24326497.v1.

[13] P. Basu and P. Kaushal, "Biomass Gasification, Pyrolysis, and Torrefaction: Practical Design, Theory, and Climate Change Mitigation, Fourth Edition," *Biomass Gasification, Pyrolysis, and Torrefaction: Practical Design, Theory, and Climate Change Mitigation, Fourth Edition*, pp. 1–681, Jan. 2023, doi: 10.1016/C2022-0-02464-8.

[14] C. F. Chang, C. Y. Chang, and W. T. Tsai, "Effects of burn-off and activation temperature on preparation of activated carbon from corn cob agrowaste by CO2 and steam," *J Colloid Interface Sci*, vol. 232, no. 1, pp. 45–49, Dec. 2000, doi: 10.1006/jcis.2000.7171.

[15] Y. Ngernyen, C. Tangsathitkulchai, and M. Tangsathitkulchai, "Porous properties of activated carbon produced from Eucalyptus and Wattle wood by carbon dioxide activation," *Korean Journal of Chemical Engineering*, vol. 23, no. 6, pp. 1046–1054, Nov. 2006, doi: 10.1007/S11814-006-0028-9/METRICS.

[16] J. R. Grace, "Contacting Modes and Behaviour Classification of Gas-Solid and Other Two-Phase Suspensions," *Can J Chem Eng*, vol. 64, no. June, pp. 353–363, 1986.

[17] C. Y. Wen and Y. H. Yu, "A generalized method for predicting the minimum fluidization velocity," *American Institute of Chemical Engineers Journal*, vol. 12, no. 3, pp. 610–612, 1966, doi: 10.1002/aic.690120343.
[18] "Analytical Methods." Accessed: Mar. 14, 2024. [Online]. Available: https://www.european-biochar.org/en/ct/8
[19] S. Brunauer, P. H. Emmett, and E. Teller, "Adsorption of Gases in Multimolecular Layers," 1938, Accessed: Mar. 14, 2024. [Online]. Available: https://pubs.acs.org/sharingguidelines
[20] J. Rouquerol, P. Llewellyn, and F. Rouquerol, "Is the bet equation applicable to microporous adsorbents?," *Stud Surf Sci Catal*, vol. 160, pp. 49–56, Jan. 2007, doi: 10.1016/S0167-2991(07)80008-5.
[21] D. Neves, H. Thunman, A. Matos, L. Tarelho, and A. Gómez-Barea, "Characterization and prediction of biomass pyrolysis products," *Prog Energy Combust Sci*, vol. 37, no. 5, pp. 611–630, Sep. 2011, doi: 10.1016/J.PECS.2011.01.001.
[22] X. Jing *et al.*, "Evaluation of CO2 gasification reactivity of different coal rank chars by physicochemical properties," *Energy and Fuels*, vol. 27, no. 12, pp. 7287–7293, 2013, doi: 10.1021/ef401639v.